Sampling-based Fast Gradient Rescaling Method for Highly Transferable Adversarial Attacks

Xu Han & Anmin Liu*& Yifeng Xiong
School of Computer Science and Technology
Huazhong University of Science and Technology
Wuhan, 430074, China
{hans,lam,xiongyf}@hust.edu.cn

Yanbo Fan
Tencent
Shenzhen, China
fanyanbo0124@gmail.com

Kun He†
School of Computer Science and Technology
Huazhong University of Science and Technology
Wuhan, 430074, China
brooklet60@hust.edu.cn

Abstract

Deep neural networks have shown to be very vulnerable to adversarial examples crafted by adding human-imperceptible perturbations to benign inputs. After achieving impressive attack success rates in the white-box setting, more focus is shifted to black-box attacks. In either case, the common gradient-based approaches generally use the $sign$ function to generate perturbations at the end of the process. However, only a few works pay attention to the limitation of the $sign$ function. Deviation between the original gradient and the generated noises may lead to inaccurate gradient update estimation and suboptimal solutions for adversarial transferability, which is crucial for black-box attacks. To address this issue, we propose a Sampling-based Fast Gradient Rescaling Method (S-FGRM) to improve the transferability of the crafted adversarial examples. Specifically, we use data rescaling to substitute the inefficient $sign$ function in gradient-based attacks without extra computational cost. We also propose a Depth First Sampling method to eliminate the fluctuation of rescaling and stabilize the gradient update. Our method can be used in any gradient-based optimizations and is extensible to be integrated with various input transformation or ensemble methods for further improving the adversarial transferability. Extensive experiments on the standard ImageNet dataset show that our S-FGRM could significantly boost the transferability of gradient-based attacks and outperform the state-of-the-art baselines.

1 Introduction

Along with their incredible success in computer vision tasks, the robustness of deep neural networks (DNNs) has also raised serious concerns. DNNs have been found to be vulnerable to adversarial examples [6, 25] crafted by introducing human-imperceptible perturbations to benign input. Worse still, adversarial examples have been demonstrated to be transferable [17, 20, 14], meaning that adversarial examples generated for one model can be used to fool other black-box models, allowing for real-world black-box attacks [33, 22].

*The first two authors contribute equally.
†Corresponding author.

Preprint. Under review.

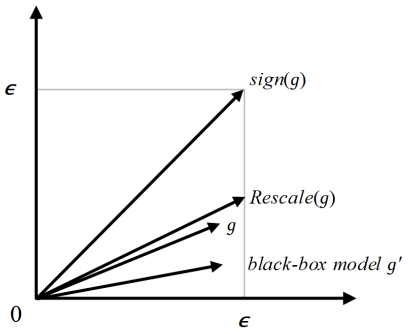

Figure 1: Illustration of the synthetic direction of $sign$ function. There do exist non-negligible deviation between $sign(g)$ and the true gradient g. In comparison, our $Rescale(g)$ has a better chance of approaching both g and g'

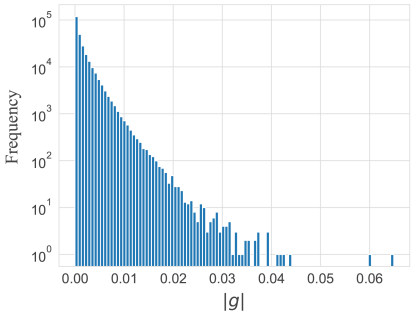

Figure 2: Distribution of the absolute true gradient values during the adversarial example generation. Most of the gradient values are extremely small and close to 0

Numerous works have been proposed to investigate the adversarial robustness of deep learning models, including gradient-based single-step methods like fast gradient sign method (FGSM) [6] and its randomized variant [26], multi-step methods like the basic iterative method (BIM) [11] and the projected gradient descent (PGD) attack [16], which is known as one of the most powerful attack methods. These adversarial attack strategies can achieve high success rates under the white-box setting, for which the attacker has access to the architecture, model parameters and any other information about the present model. However, they often exhibit low success rates under the black-box setting.

Many recent efforts have attempted to further improve the transferability of adversarial examples in order to address the challenge of black-box setting, including gradient optimization attacks [11, 2, 13, 29], input transformation attacks [32, 3, 13] and model ensemble attacks [2, 14]. Gradient optimization attacks attempt to boost black-box performance by advanced gradient calculation. Input transformation attacks aim to find adversarial perturbations with higher transferability by applying various transformations to the inputs. By fusing the logit outputs, model ensemble attacks generate adversarial examples on multiple models simultaneously. The latter two categories are both based on existing gradient-based attacks to further boost the transferability.

Among these schemes, little attention has been paid to the widely used basic gradient approach using the $sign$ function. The $sign$ function guarantees an l_∞ bound on the gradient update, as well as sufficient perturbations and a somewhat proper update direction, making it successful and being widely adopted in most gradient optimization methods. We observe that, however, the $sign$ function could not offer an accurate approximation on the gradient update direction, resulting in just two values of ± 1 in most cases (the value of 0 rarely happens for the real value of gradients). For instance, if the actual gradient in two dimensions is $(0.8, 10^{-8})$, the sign gradient will be $(1, 1)$ but $(1, 0)$ is a more accurate approximation. For another example, as illustrated in Figure 1 in two dimensions, where ϵ is the perturbation budget for the current update, the update direction provided by $sign$ deviates from the direction of both the original gradient and black-box model's gradient. We argue that such inaccuracy may harm the adversarial transferability.

Based on the aforementioned analysis, we propose a Sampling-based Fast Gradient Rescaling Method (S-FGRM) to have a more accurate gradient approximation and increase the transferability of gradient-based attacks. We design a data rescaling method for the gradient computation, that directly exploits the distribution of gradient values in different dimensions and maintains their disparities. Moreover, as most gradient values are extremely small, as shown in Figure 2, we introduce a sampling method, dubbed Depth First Sampling, to stabilize the update direction. Our sampling method eliminates the local fluctuation error and further boosts the transferability of the crafted examples. Note that our proposed method is generally applicable to any gradient-based attacks and can be combined with a variety of input transformation or ensemble methods to further enhance the adversarial transferability.

Extensive experiments and analysis show that our integrated methods mitigate the overfitting issue and further strengthen various gradient-based attacks.

2 Related Work

2.1 Adversarial Attacks

Adversarial attacks can be roughly divided into two categories: white-box attacks and black-box attacks. Due to the lack of model information, attacks in black-box setting are more challenging than in white-box setting. Since the decision boundaries between models are similar, one popular approach for black-box attacks is to generate adversarial examples from substitute models and then transfer them into target models. Many concrete methods [29, 32, 3, 13, 35, 30, 27] based on adversarial transferability [25] have been proposed, which can be classified into three categories: gradient optimization attacks, input transformation attacks and model ensemble attacks.

Gradient Optimization Attacks. Goodfellow *et al*. [6] propose Fast Gradient Sign Method (FGSM) with an update step size equals to the perturbation boundary, replacing the actual gradient with the output of *sign* function. Kurakin *et al*. [11] propose I-FGSM as an iterative version of FGSM [6], which iterates FGSM with a smaller step size, thus increasing white-box attack success but decreasing transferability. To improve the transferability of crafted adversarial examples, Dong *et al*. [2] integrate the momentum method into I-FGSM, namely MI-FGSM, to maintain high transferability. By inserting the velocity vector in the gradient of the input, it helps to alleviate poor local maximum and stabilize the update direction. Lin *et al*. [13] further propose NI-FGSM that employ Nesterov's accelerated gradient (NAG)[19] to escape the poor local maximum faster from a perspective of optimization. Due to the anticipation property of NAG, NI-FGSM can look ahead to have a more accurate update direction. On the other hand, Wu *et al*. [29] take the local gradient fluctuation into account and develop vr-FGSM. It utilizes the variance-reduced gradient, covering information of the area around the benign input. Wang *et al*. [27] propose Variance Tuning (VT), using the previous gradient variance to tune the current gradient calculation at each iteration. They both try to reduce the variance of the gradient to have a more stable update direction.

Input Transformation Attacks. Apart from the gradient optimization, another line of boosting the adversarial transferability is input transformation. Xie *et al*. [32] propose the Diverse Input Method (DIM) that applies random input transformation with fixed probability to alleviate the overfitting trend of I-FGSM, resulting in high attack success rate under both white-box and black-box settings. Dong *et al*. [3] propose the Translation Invariant Method (TIM) to mitigate the white-box model's sensitivity on adversarial examples by using a set of translated images. Holding the assumption of translation-invariant property, the pre-defined kernel in TIM reduces the computational cost greatly while generating more model-independent adversarial examples. Lin *et al*. [13] propose conceptions of loss-preserving transformation and model augmentation. They present the Scale-Invariant Method (SIM) and also validate the scale-invariant property empirically. By analogizing the scale transformation to model augmentation, SIM optimizes the adversarial perturbations and generates robust and transferable adversarial examples. Wang *et al*. [28] propose Admix that uses the original label of the input to create more transferable adversaries by calculating the gradient on the input image admixed with a small portion of each add-in image.

2.2 Adversarial Defenses

On the other hand, many adversarial defense methods have been proposed to protect the models from being fooled by adversarial examples.

Adversarial training based defenses. Adversarial training is one of the most powerful and effective defense methods, which augments the training data by generating adversarial examples during the training process. Goodfellow *et al*. [6] discover that by adding adversarial examples for model training could improve the model robustness. Madry *et al*. [16] apply their projected gradient descent (PGD) to adversarial training to gain a significant increment on the robustness of trained models. Tramèr *et al*. [26] propose ensemble adversarial training, which augments the training data with perturbations generated by several models. Recently, Gong *et al*. [5] propose a lightweight variant of adversarial training called MaxUp, that is simpler and faster.

Input transformation based defenses. In addition to adversarial training, input transformation and feature preprocessing are also proposed to defend against the adversarial attacks. Xie *et al*. [31] add a randomization layer including random resizing and padding to models, mitigating the adversarial effects. Xu *et al*. [34] reduce the search space of adversarial perturbation by feature squeeze. Guo *et al*. [7] apply image transformations such as JPEG compression and image quilting to training the models. Liao *et al*. [12] propose high-level representation guided denoiser (HGD), improving the robustness against both white-box and black-box attacks. Liu *et al*. [15] propose a JPEG-based defensive compression framework called feature distillation (FD) to guarantee the defense efficiency as well as classification accuracy on benign data. Jia *et al*. [10] propose an end-to-end image compression model dubbed ComDefend to improve the robustness against attacks efficiently. Naseer *et al*. [18] combine adversarial training with input processing and train a purified model called Neural Representation Purifier (NPR).

3 Methodology

In this section, we first introduce the family of gradient-based attack methods in Sec. 3.1, then we illustrate our motivation in Sec. 3.2 and introduce the two key components of our method in Sec. 3.4 and Sec. 3.3, respectively. In the end, we provide the detailed description on the proposed Sampling-based Fast Gradient Rescaling Method (S-FGRM) in Sec. 3.5.

3.1 Gradient-based Attack Methods

Gradient-based methods are the mainstream of adversarial attacks and they also server as the base method of other types of adversarial attacks. In this work, we mainly focus on the attack transferability and integrate our method with the following typical gradient-based attacks.

Fast Gradient Sign Method (FGSM) [6] is the most early single-step method for generating adversarial examples:

$$x^{adv} = x + \epsilon \cdot \text{sign}(\nabla_x J(x, y)), \tag{1}$$

where $\nabla_x J(x, y)$ is the gradient of the loss function w.r.t. x.

Momentum Iterative Fast Gradient Sign Method (MI-FGSM) [2] introduce the momentum into I-FGSM to boost the adversarial attacks:

$$\begin{aligned} g_{t+1} &= \mu g_t + \frac{\nabla_{x_t^{adv}} J(x_t^{adv}, y)}{||\nabla_{x_t^{adv}} J(x_t^{adv}, y)||_1}, \\ x_{t+1}^{adv} &= x_t^{adv} + \alpha \cdot \text{sign}(g_{t+1}), \end{aligned} \tag{2}$$

where $g_0 = 0, x_0^{adv} = x$ and μ is a decay factor.

Nesterov Iterative Fast Gradient Sign Method (NI-FGSM) [13] proposes to integrate Nesterov's accelerated gradient into the iterative attack to further improve the transferability:

$$\begin{aligned} x_t^{nes} &= x_t^{adv} + \alpha \cdot \mu \cdot g_t, \\ g_{t+1} &= \mu \cdot g_t + \frac{\nabla_{x_t^{nes}} J(x_t^{nes}, y^{true})}{||\nabla_{x_t^{nes}} J(x_t^{nes}, y^{true})||_1}, \\ x_{t+1}^{adv} &= x_t^{adv} + \alpha \cdot \text{sign}(g_{t+1}). \end{aligned} \tag{3}$$

3.2 Motivation

In the process of generating adversarial examples, gradient-based methods typically use the *sign* function to obtain the gradient estimation. Since the first gradient-based approach of Fast Gradient Sign Method (FGSM) [6], most researches take it for granted that the *sign* function is necessary and unalterable. Many studies have concentrated on the attack strategy to generate more efficient and transferable adversarial examples based on FGSM. The procedure of generating perturbations that relies on *sign* has received little attention.

However, we find that such an operation has side effects, especially on the direction of gradient update. The synthetic directions associated with each gradient value are limited since the output

of the *sign* function is either 0 or ± 1. With no doubt, and 0 rarely happens for the true gradient values. Using *sign* will result in an imprecise estimate on the gradient. As can be seen intuitively from Figure 1, the angle between *sign*(g) and *black-box model g'* is much larger. Based on the above analysis, we attempt to directly employ the distribution of the initial gradient by simply introducing the data rescaling method to the last step. It will retain the difference between the gradient values, which mostly influences the synthetic direction, as compared to the original *sign* function. Our **Fast Gradient Rescaling Method** is straightforward but effective, with little computational overhead.

To our knowledge, one of the functions of $sign$ is to produce enough perturbations. Without $sign$, even a tiny numerical inaccuracy might create a huge difference in the rescaling results due to the minimal values of the gradient. To compensate for this deficiency, we propose our **Depth First Sampling Method**. By sampling around the input image, the negative influence of small value fluctuations will be alleviated. Unlike typical sampling methods, starting with the second sampling, we sample around the previous sampled image rather than the original input image. This strategy is similar to depth-first search. It not only mitigates rescaling uncertainty but also investigates model decision boundaries, which reduces overfitting to some extent and improves the attack transferability. Then, we propose our **Sampling-based Fast Gradient Rescaling Method (S-FGRM)** to further enhance the adversarial transferability by combining these two methods.

3.3 Fast Gradient Rescaling Method

Typical gradient-based adversarial attack methods, like I-FGSM, MI-FGSM, NI-FGSM, *etc*., are inextricably linked to the $sign$ function. There is no doubt that the $sign$ function provides sufficient perturbation for the gradient update, allowing crafted adversarial examples to get close to their targeted class more easily. Despite this, it is not the optimal solution. The synthetic directions produced by $sign$ are limited, as we have illustrated in Figure 1, which influences the speed of gradient convergence as well as the transferability. Gao *et al*. [4] also observed the limitation of $sign$. They sorted all the gradient units and assigned them with values designated for intervals. Their method sharply slows down the generation of adversarial examples, which is not applicable in most complex scenarios. To develop a simple yet more efficient method, we introduce data rescaling into the gradient update and define the gradient rescaling equation as follows:

$$
\begin{aligned}
Rescale(g) &= ln(1 + \textit{min-max}\,(-\log_2 \mid g \mid)), \\
\textit{min-max}\,(x_i^{'}) &= \frac{x_i - \min\limits_{1 \le j \le n} \{x_j\}}{\max\limits_{1 \le j \le n} \{x_j\} - \min\limits_{1 \le j \le n} \{x_j\}}.
\end{aligned} \tag{4}
$$

We utilize the logarithm of $\mid g \mid$ to base 2 and represent the fractional part of the gradient values in binary, thus the closely distributed values will be scattered. The original gradient is linearly transformed through the min-max standardization, and the value is mapped between $[0, 1]$. Data smoothing is performed at the end of the equation by mapping the intermediate result on $ln(1 + x)$. Compared with Staircase [4], our gradient rescaling method is more straightforward and more effective without a large computational expense on the sorting.

3.4 Depth First Sampling Method

In order to stabilize the effect of gradient rescaling, we adopt sampling to remove the local fluctuation. Wu *et al*. [29] substitute each gradient with an averaged one during the iterations to alleviate the shattering of gradients. Inspired by the logic of depth-first search, we propose **Depth First Sampling Method**. We define the potential samples around sampled images as their neighbors. Instead of just sampling around the input images, we also take their neighbors into consideration. As illustrated in Figure 3, when a sampling operation is completed, the next sampling center will shift to the point just sampled. Specifically, given a classifier f with loss function J and input image $x \in \mathcal{X}$, our depth first sampling strategy is designed as follows:

$$
g_t = \frac{1}{N+1} \sum_{i=0}^{N} \nabla J(x_t^i, y; \theta), \quad x_t^{i+1} = x_t^i + \xi_i. \tag{5}
$$

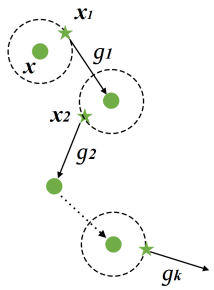

Figure 3: Illustration of the Depth First Sampling Method. Here x represents the input image of the current iteration. Each sampling operation is performed on the previous sampled point. The average gradient of g_k is accumulated to further boost the transferability

Algorithm 1 SMI-FGRM

Input: A classifier f with loss function J, parameters θ; a benign example x with ground-truth label y
Input: The maximum perturbation ϵ; number of iterations T
Input: The number of sampling N
Output: Adversarial example x^{adv}

Initialize: $\alpha = \epsilon/T$, $x_0^{adv} = x$, $g_0 = 0$
for $t = 0$ to $T-1$ **do**
    Calculate the sampled gradient $\hat{g}_{t+1}$ by Eq. 5
    Update g_{t+1} by momentum
        $g_{t+1} = \mu \cdot g_t + \frac{\hat{g}_{t+1}}{\|\hat{g}_{t+1}\|_1}$
    Update x_{t+1}^{adv} by applying the gradient rescaling method
        $x_{t+1}^{adv} = x_t^{adv} + \alpha \cdot Rescale(g_{t+1})$
end for
$x^{adv} = x_T^{adv}$
return x^{adv}

Here $x_t^0 = x$, $\xi_i \sim U[-(\beta \cdot \epsilon)^d, (\beta \cdot \epsilon)^d]$. N is the sampling number. ϵ is the maximum perturbation in the current iteration and β is a hyperparameter that determines the sampling range. By accumulating the gradient of sampled examples and benign image, the fluctuation effect is expected to be weakened while the transferability of the crafted examples will be enhanced.

3.5 Sampling-based Fast Gradient Rescaling Method

To gain a better grasp of our entire methodology, we incorporate the proposed method into MI-FGSM, denoted as Sampling-based Momentum Iterative Fast Gradient Rescaling Method (SMI-FGRM). Specific details are described in Algorithm 1. Similarly, we could incorporate the proposed method into NI-FGSM, and obtain an enhanced method SNI-FGRM. Any gradient-based attacks can get benefit from our S-FGRM.

4 Experiments

To demonstrate the effectiveness of our S-FGRM, we conduct extensive experiments in this section. We start with the experimental setup, then make a comparison with typical gradient-based attacks in a variety of attack settings, following the evaluation on nine advanced defense models. In the end, we report ablation studies on the hyper-parameters.

4.1 Experimental Setup

Dataset. The dataset used for evaluation is from the ImageNet that contains 1000 images randomly picked from the ILSVRC 2012 validation set [21], which is widely used in recent gradient-based attacks [2, 13, 27].

Table 1: Attack success rates (%) of adversarial attacks on seven models in the single model setting. The adversarial examples are crafted on Inc-v3, Inc-v4, IncRes-v2, and Res-101 respectively. * indicates the white-box model

Model	Attack	Inc-v3	Inc-v4	IncRes-v2	Res-101	Inc-v3$_{ens3}$	Inc-v3$_{ens4}$	IncRes-v2$_{ens}$
Inc-v3	MI-FGSM	**100.0***	44.3	42.4	36.2	13.8	13.0	6.6
	SMI-FGRM	**100.0***	**83.5**	**81.9**	**73.6**	**39.2**	**37.3**	**19.4**
	NI-FGSM	**100.0***	51.3	49.9	40.6	12.8	12.9	6.6
	SNI-FGRM	**100.0***	**84.8**	**84.5**	**76.6**	**39.4**	**36.8**	**19.0**
Inc-v4	MI-FGSM	55.3	**99.7***	46.0	40.7	16.6	15.4	7.6
	SMI-FGRM	**88.4**	99.6*	**83.7**	**78.3**	**51.3**	**47.6**	**31.4**
	NI-FGSM	63.4	**100.0***	52.4	45.0	15.5	14.3	6.9
	SNI-FGRM	**90.8**	99.8*	**85.5**	**79.0**	**51.6**	**48.2**	**29.4**
IncRes-v2	MI-FGSM	58.6	50.0	98.0*	46.0	21.2	16.1	10.7
	SMI-FGRM	**87.1**	**85.1**	**98.3***	**80.4**	**58.8**	**52.6**	**42.1**
	NI-FGSM	64.1	54.1	99.0*	45.3	20.2	14.9	10.0
	SNI-FGRM	**89.1**	**87.7**	**99.1***	**81.3**	**61.2**	**50.9**	**42.2**
Res-101	MI-FGSM	58.4	51.4	49.2	99.3*	23.8	21.3	12.8
	SMI-FGRM	**85.7**	**81.7**	**81.8**	**99.8***	**59.2**	**55.1**	**40.6**
	NI-FGSM	65.5	59.8	56.0	99.4*	23.5	20.5	11.4
	SNI-FGRM	**86.9**	**83.1**	**83.1**	**99.8***	**60.4**	**55.2**	**40.5**

Models. We conduct our experiments on seven state-of-the-art models, including four normally trained models: Inception-v3 (Inc-v3) [24], Inception-v4(Inc-v4), Inception-Resnet-v2(IncRes-v2) [23], Resnet-v2-101 (Res-101) [9], and three adversarially trained models: Inc-v3$_{ens3}$, Inc-v3$_{ens4}$ and IncRes-v2$_{ens}$ [26]. Moreover, we include nine advanced defense models: HGD [12], R&P [31], NIPS-r3, Bit-Red [34], JPEG [8], FD [15], ComDefend [10], RS [1] and NRP [18].

Baselines. To verify the effectiveness of our methods, we select two popular gradient-based attack methods as the baselines, *i.e*. MI-FGSM and NI-FGSM. Besides, we compare the proposed method with a common sampling method, namely variance-reduced attack [29]. We also integrate our methods with up-to-date input transformations, including DIM [32], TIM [3], SIM and CTM [13], to show the improvement on performance. Our boosted methods are denoted as SM(N)I-DI-FGRM, SM(N)I-TI-FGRM, SM(N)I-SI-FGRM, SM(N)I-CT-FGRM, respectively.

Hyperparameters. We follow the prior settings for hyper-parameters [2]. We set the maximum perturbation $\epsilon = 16$ with the pixel values normalized to interval [0,1], the number of iterations $T = 10$ and step size $\alpha = 1.6$. We adopt the default decay factor $\mu = 1.0$ for MI-FGSM and NI-FGSM. The transformation probability of DIM is set to 0.5. We adopt the Gaussian kernel with kernel size 7×7 for TIM. The number of scale copies is set to 5 for SIM. For vr-FGSM, as the optimal σ varies for different models, we set the standard deviation $\sigma = 15.0$ within their optimal interval that the authors provided. For our method, the parameters for sampling are set to $N = 12$, $\beta = 1.5$.

4.2 Attack a Single Model

We first perform four adversarial attacks, including MI-FGSM, NI-FGSM, the proposed SNI-FGRM and SMI-FGRM on a single model to test the transferability. In this experiment, we generate adversarial examples on the first four normally trained networks respectively and evaluate them on the seven neural networks mentioned above. The attack success rates are presented in Table 1. SMI-FGRM and SNI-FGRM maintain nearly 100% success rates under the white-box setting. For black-box attacks, they also surpass MI-FGSM and NI-FGSM by a large margin. For example, on the first and second rows, we craft adversarial examples on Inc-v3 model. Our proposed SMI-FGRM achieves 83.5% success rate on Inc-v4 and 39.2% success rate on Inc-v3$_{ens}$ while MI-FGSM only gets 44.3% and 13.8% corresponding success rates. The results demonstrate that S-FGRM boosts the two gradient-based methods significantly and enhances the attack transferability.

Table 2: Attack success rates (%) of adversarial attacks on seven models in the single model setting with input transformations. The adversarial examples are crafted on Inc-v3, Inc-v4, IncRes-v2, and Res-101 respectively. * indicates the white-box model

Model	Attack	Inc-v3	Inc-v4	IncRes-v2	Res-101	Inc-v3$_{ens3}$	Inc-v3$_{ens4}$	IncRes-v2$_{ens}$
Inc-v3	MI-CT-FGSM	99.4*	84.0	81.5	78.1	68.2	64.2	46.2
	vrMI-CT-FGSM	99.2*	86.9	86.6	83.4	86.3	85.6	76.5
	SMI-CT-FGSM(**Ours**)	99.1*	91.4	90.4	86.6	86.7	85.8	76.7
	SMI-CT-FGRM(**Ours**)	**99.6***	**92.6**	**91.9**	**88.3**	**87.3**	**86.0**	**77.3**
	NI-CT-FGSM	99.3*	84.6	81.6	74.3	60.6	56.2	41.1
	vrNI-CT-FGSM	99.2*	86.9	85.9	83.9	86.0	86.0	77.0
	SNI-CT-FGSM(**Ours**)	99.5*	92.7	91.8	89.2	**87.1**	**87.2**	77.4
	SNI-CT-FGRM(**Ours**)	**99.8***	**94.0**	**92.7**	**89.7**	**87.1**	86.9	**77.5**
Inc-v4	MI-CT-FGSM	87.0	99.1*	84.1	78.6	70.4	69.1	58.0
	vrMI-CT-FGSM	89.1	98.4*	84.0	81.4	84.8	83.8	77.2
	SMI-CT-FGSM(**Ours**)	91.8	99.1*	89.4	86.4	86.1	**86.4**	80.0
	SMI-CT-FGRM(**Ours**)	**94.8**	**99.8***	**92.0**	**88.7**	**88.4**	86.3	**80.3**
	NI-CT-FGSM	87.6	99.5*	81.9	77.0	66.7	61.5	49.6
	vrNI-CT-FGSM	87.7	98.3*	84.1	81.1	85.0	83.7	77.7
	SNI-CT-FGSM(**Ours**)	93.5	99.4*	90.3	85.5	87.2	86.5	**80.3**
	SNI-CT-FGRM(**Ours**)	**94.9**	**99.7***	**92.7**	**87.8**	**88.7**	**87.4**	79.0
IncRes-v2	MI-CT-FGSM	88.1	86.7	97.2*	82.2	77.5	75.5	72.0
	vrMI-CT-FGSM	87.1	84.8	97.0*	84.6	87.6	87.0	84.4
	SMI-CT-FGSM(**Ours**)	90.2	89.5	97.7*	87.4	88.6	87.4	85.9
	SMI-CT-FGRM(**Ours**)	**94.6**	**92.8**	**99.1***	**91.7**	**90.7**	**89.8**	**88.7**
	NI-CT-FGSM	90.6	87.8	99.3*	83.4	74.1	68.3	64.4
	vrNI-CT-FGSM	88.0	86.3	97.5*	85.0	88.1	86.2	85.7
	SNI-CT-FGSM(**Ours**)	92.2	91.8	99.1*	89.1	89.3	88.1	87.1
	SNI-CT-FGRM(**Ours**)	**94.7**	**94.3**	**99.5***	**91.0**	**91.5**	**90.5**	**87.9**
Res-101	MI-CT-FGSM	85.7	82.0	82.4	98.5*	76.1	71.1	61.6
	vrMI-CT-FGSM	81.9	73.0	78.5	99.1*	86.5	84.1	78.6
	SMI-CT-FGSM(**Ours**)	86.8	81.2	85.2	98.7*	86.8	85.2	81.1
	SMI-CT-FGRM(**Ours**)	**90.1**	**83.2**	**88.2**	**99.7***	**89.7**	**87.1**	**83.2**
	NI-CT-FGSM	87.3	83.2	85.6	99.1*	73.2	66.8	56.0
	vrNI-CT-FGSM	81.5	71.5	78.2	98.7*	85.2	83.7	77.2
	SNI-CT-FGSM(**Ours**)	87.6	82.6	86.1	**99.7***	88.2	85.8	81.6
	SNI-CT-FGRM(**Ours**)	**89.4**	**83.3**	**88.2**	99.5*	**89.2**	**87.3**	**82.7**

4.3 Attack with Input Transformations

Lin *et al*. [13] have demonstrated that the Composite Transformation Method (CTM), combined by the most state-of-the-art input transformations, including DIM, TIM and SIM, improve the transferability of adversarial examples significantly. Therefore, in this subsection, we integrate our S-FGRM with CTM to further boost the transferability of gradient-based attacks. Besides, we also take vr-FGSM as a baseline and set the sampling number $N = 20$ to gain this method's best performance and show the superiority of our method. As depicted in Table 2, our SMI-CT-FGRM and SNI-CT-FGRM consistently outperform the baseline methods by $10\% \sim 36\%$. The average improvements of SMI-CT-FGRM over vrMI-CT-FGSM are about $5\% \sim 12\%$ as the same for SNI-CT-FGRM over vrNI-CT-FGSM. Comparing SM(N)I-CT-FGRM with SM(N)I-CT-FGSM alone, we can observe that our Fast Gradient Rescaling Method further improves the transferability by about 2%. The great performance stated above convincingly validates the effectiveness of proposed S-FGRM.

4.4 Attack an Ensemble of Models

In this subsection, we follow the ensemble attack settings in [2]. We integrate our S-FGRM with the ensemble attack method to show that S-FGRM is capable of improving the transferability under multi-model setting. We craft adversarial examples on the ensemble of four normally trained models, *i.e*., Inc-v3, Inc-v4, IncRes-v2 and Res-101, with averaged logit outputs. As summarized in Table 3, our S-FGRM has better performance than the baseline attacks. It is worth noting that the proposed method improves the transferability of the baselines by more than 49% for MI-FGSM and 53% for NI-FGSM. In addition, when combined with CTM, S-FGRM boosts MI-CT-FGSM and NI-CT-FGSM on adversarially trained models by 6.6% and 8.4%, respectively.

Table 3: Attack success rates (%) on seven models in the ensemble-model setting. The adversarial examples are crafted on the ensemble model including Inc-v3, Inc-v4, IncRes-v2 and Res-101

Attack	Inc-v3	Inc-v4	IncRes-v2	Res-101	Inc-v3$_{ens3}$	Inc-v3$_{ens4}$	IncRes-v2$_{ens}$
MI-FGSM	**100.0***	99.6*	99.5*	99.9*	47.9	43.1	27.9
SMI-FGRM	**100.0***	**99.8***	**99.7***	**99.9***	**88.7**	**87.5**	**77.0**
NI-FGSM	**100.0***	**99.9***	99.9*	**100.0***	46.8	41.9	24.8
SNI-FGRM	**100.0***	**99.9***	**100.0***	99.9*	**88.8**	**87.3**	**78.2**
MI-CT-FGSM	99.7*	98.8*	97.6*	99.9*	91.6	89.8	86.5
SMI-CT-FGRM	**99.9***	**99.7***	**99.7***	**100.0***	**97.0**	**96.4**	**94.4**
NI-CT-FGSM	99.8*	**99.9***	99.3*	**99.9***	92.3	89.7	84.4
SNI-CT-FGRM	**100.0***	**99.9***	**100.0***	**99.9***	**98.4**	**97.5**	**95.8**

Table 4: Attack success rates (%) of adversarial attacks on nine models with advanced defense mechanism

Model	Attack	HGD	R&P	NIPS-r3	Bit-Red	JPEG	FD	ComDefend	RS	NRP	Average
Inc-v3	MI-CT-FGSM	57.9	46.1	54.4	45.3	76.1	71.4	79.2	27.6	41.7	55.5
	SMI-CT-FGRM	**76.6**	**70.8**	**78.3**	**67.7**	**88.1**	**85.0**	**90.4**	**44.0**	**67.1**	**74.2**
	NI-CT-FGSM	49.3	40.5	49.0	42.7	72.3	68.4	79.4	25.4	34.9	51.3
	SNI-CT-FGRM	**77.3**	**72.2**	**79.1**	**65.4**	**90.3**	**84.8**	**90.1**	**44.9**	**68.1**	**74.7**
Ens	MI-CT-FGSM	90.6	88.0	89.8	77.1	93.6	89.6	94.7	46.9	75.6	82.9
	SMI-CT-FGRM	**95.2**	**94.1**	**95.5**	**86.6**	**98.4**	**94.8**	**98.0**	**69.9**	**87.7**	**91.1**
	NI-CT-FGSM	90.8	85.3	89.1	72.0	96.1	89.0	95.4	43.5	70.3	81.3
	SNI-CT-FGRM	**96.5**	**95.4**	**96.3**	**87.8**	**99.2**	**95.6**	**99.0**	**70.2**	**88.9**	**92.1**

4.5 Attack Advanced Defense Models

To further verify the effectiveness of our methods, we carry out the evaluations on nine models with advanced defense strategies, including the top-3 defense solutions in the NIPS competition (HGD(rank-1) [12], R&P(rank-2) [31], NIPS-r3(rank-3)) and six recently proposed defense models (Bit-Red [34], JPEG [8], FD [15], ComDefend [10], RS [1] and NRP [18]). The results are organized in Table 4. Notably, in the single model setting, our methods yield an average attack success rate of 74.2% for SMI-CT-FGRM and 74.7% for SNI-CT-FGRM on Inc-v3 model, outperforming the baselines for more than 18% and 23%. In the multi-model setting, our methods achieve an average attack success rate of 91.1% for SMI-CT-FGRM and 92.1% for SNI-CT-FGRM. The consistent improvement shows great effectiveness and generalization of our S-FGRM for gradient-based attacks to achieve higher transferability.

4.6 Ablation Study

We conduct a series of ablation studies to investigate the impact of the hyper-parameters in S-FGRM. Here, we tune N and β respectively and test the transferability of the adversaries on Inc-v3 model without input transformations.

4.6.1 On the number of sampled examples *N*.

We first analyze the effectiveness of the sampling number N on the attack success rate of S-FGRM. We integrate S-FGRM with MI-FGSM and NI-FGSM, respectively. The parameter of the sampling range β is fixed to 3/2. We tune $N = 0, 1, 2, ..., 22$. When $N = 0$, SMI-FGRM and SNI-FGRM degrade to MI-FGRM and NI-FGRM, respectively. The results are shown in Figure 4. As the value of N increases, the black-box attack success rate increases rapidly and reaches the peak at about $N = 12$. We take $N = 12$ as the relatively optimal parameter in experiments since a bigger value of N leads to a higher computational overhead.

4.6.2 On the size of sampling range β.

We then study the impact of the sampling range β. Similarly, we apply our S-FGRM to MI-FGSM and NI-FGSM, respectively, fix $N = 12$, and let β range from 0 to 3. $\beta = 0$ denotes the corresponding FGRM. As shown in Figure 5, with the increment of the sampling range, the black-box success rate

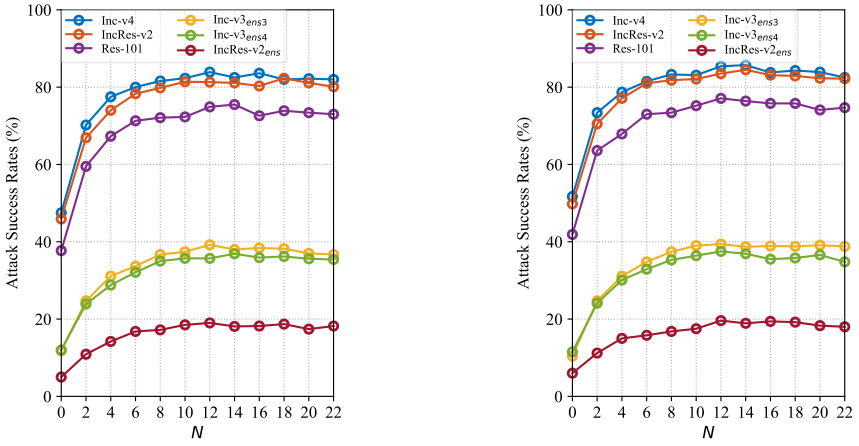

Figure 4: The attack success rates (%) on the other six models with adversarial examples generated by SMI-FGRM (left) and SNI-FGRM (right) on Inc-v3 model for various sampling numbers

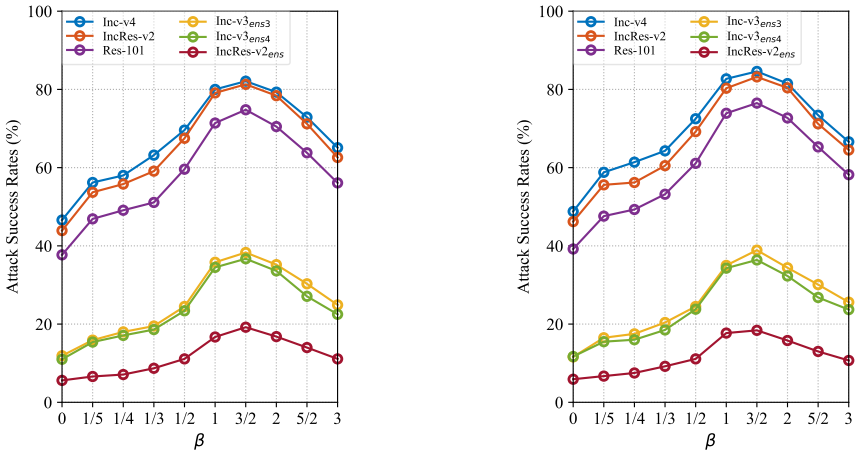

Figure 5: The attack success rates (%) on the other six models with adversarial examples generated by SMI-FGRM (left) and SNI-FGRM (right) on Inc-v3 model for various sampling ranges

increases and remains stable after β exceeds 1.5. When $\beta > 1.5$, the performance decays gradually. Therefore, we set the sampling range $\beta = 1.5$ in the experiments.

5 Conclusions

In this work, we revisit the basic operation of the $sign$ function in gradient-based adversarial attack methods, and discuss its limitations caused by the inaccurate approximation of the true gradient values. Based on our observations, we propose a simple yet more efficient method called the Sampling-based Fast Gradient Rescaling Method (S-FGRM) to enhance the adversarial transferability for black-box attacks. Specifically, we introduce data rescaling to the gradient update and remove the local fluctuation by depth first sampling. In this way, S-FGRM can further improve the adversarial transferability. We then incorporate our method into typical gradient-based attacks. Our methods surpass the vanilla MI-FGSM and NI-FGSM by a large margin. Even when compared with variance-reduced attack, our method also exhibits its superiority. Extensive experiments validate our method's efficiency and broad applicability.

Acknowledgements

This work is supported by National Natural Science Foundation of China (62076105) and International Cooperation Foundation of Hubei Province, China (2021EHB011).

References

[1] Jeremy Cohen, Elan Rosenfeld, and Zico Kolter. Certified adversarial robustness via randomized smoothing. In *Proceedings of the 36th International Conference on Machine Learning, ICML*, pages 1310–1320, 2019.

[2] Yinpeng Dong, Fangzhou Liao, Tianyu Pang, Hang Su, Jun Zhu, Xiaolin Hu, and Jianguo Li. Boosting adversarial attacks with momentum. In *2018 IEEE Conference on Computer Vision and Pattern Recognition, CVPR*, 2018.

[3] Yinpeng Dong, Tianyu Pang, Hang Su, and Jun Zhu. Evading defenses to transferable adversarial examples by translation-invariant attacks. In *IEEE Conference on Computer Vision and Pattern Recognition, CVPR*, pages 4312–4321, 2019.

[4] Lianli Gao, Qilong Zhang, Xiaosu Zhu, Jingkuan Song, and Heng Tao Shen. Staircase sign method for boosting adversarial attacks. *arXiv preprint arXiv:2104.09722*, 2021.

[5] Chengyue Gong, Tongzheng Ren, Mao Ye, and Qiang Liu. Maxup: Lightweight adversarial training with data augmentation improves neural network training. In *IEEE Conference on Computer Vision and Pattern Recognition, CVPR*, 2021.

[6] Ian J. Goodfellow, Jonathon Shlens, and Christian Szegedy. Explaining and harnessing adversarial examples. In *3rd International Conference on Learning Representations, ICLR*, 2015.

[7] Chuan Guo, Mayank Rana, Moustapha Cissé, and Laurens van der Maaten. Countering adversarial images using input transformations. In *6th International Conference on Learning Representations, ICLR*, 2018.

[8] Chuan Guo, Mayank Rana, Moustapha Cisse, and Laurens van der Maaten. Countering adversarial images using input transformations. In *6th International Conference on Learning Representations, ICLR*, 2018.

[9] Kaiming He, Xiangyu Zhang, Shaoqing Ren, and Jian Sun. Deep residual learning for image recognition. In *IEEE Conference on Computer Vision and Pattern Recognition, CVPR*, pages 770–778, 2016.

[10] Xiaojun Jia, Xingxing Wei, Xiaochun Cao, and Hassan Foroosh. Comdefend: An efficient image compression model to defend adversarial examples. In *IEEE Conference on Computer Vision and Pattern Recognition, CVPR*, pages 6084–6092, 2019.

[11] Alexey Kurakin, Ian Goodfellow, Samy Bengio, et al. Adversarial examples in the physical world. In *5th International Conference on Learning Representations, ICLR*, 2017.

[12] Fangzhou Liao, Ming Liang, Yinpeng Dong, Tianyu Pang, Xiaolin Hu, and Jun Zhu. Defense against adversarial attacks using high-level representation guided denoiser. In *IEEE Conference on Computer Vision and Pattern Recognition, CVPR*, pages 1778–1787, 2018.

[13] Jiadong Lin, Chuanbiao Song, Kun He, Liwei Wang, and John E Hopcroft. Nesterov accelerated gradient and scale invariance for adversarial attacks. In *8th International Conference on Learning Representations, ICLR*, 2020.

[14] Yanpei Liu, Xinyun Chen, Chang Liu, and Dawn Song. Delving into transferable adversarial examples and black-box attacks. In *5th International Conference on Learning Representations, ICLR*, 2017.

[15] Zihao Liu, Qi Liu, Tao Liu, Nuo Xu, Xue Lin, Yanzhi Wang, and Wujie Wen. Feature distillation: Dnn-oriented jpeg compression against adversarial examples. In *IEEE Conference on Computer Vision and Pattern Recognition, CVPR*, pages 860–868, 2019.

[16] Aleksander Madry, Aleksandar Makelov, Ludwig Schmidt, Dimitris Tsipras, and Adrian Vladu. Towards deep learning models resistant to adversarial attacks. In *6th International Conference on Learning Representations, ICLR*, 2018.

[17] Seyed-Mohsen Moosavi-Dezfooli, Alhussein Fawzi, Omar Fawzi, and Pascal Frossard. Universal adversarial perturbations. In *IEEE Conference on Computer Vision and Pattern Recognition, CVPR*, pages 1765–1773, 2017.

[18] Muzammal Naseer, Salman Khan, Munawar Hayat, Fahad Shahbaz Khan, and Fatih Porikli. A self-supervised approach for adversarial robustness. In *IEEE/CVF Conference on Computer Vision and Pattern Recognition, CVPR*, pages 262–271, 2020.

[19] Yurii Nesterov. A method for unconstrained convex minimization problem with the rate of convergence o(1/k^2). In *Doklady AN USSR*, volume 269, pages 543–547, 1983.

[20] Nicolas Papernot, Patrick McDaniel, Ian Goodfellow, Somesh Jha, Z Berkay Celik, and Ananthram Swami. Practical black-box attacks against machine learning. In *Proceedings of the 2017 ACM on Asia Conference on Computer and Communications Security*, pages 506–519, 2017.

[21] Olga Russakovsky, Jia Deng, Hao Su, Jonathan Krause, Sanjeev Satheesh, Sean Ma, Zhiheng Huang, Andrej Karpathy, Aditya Khosla, Michael Bernstein, et al. Imagenet large scale visual recognition challenge. *International Journal of Computer Vision*, 115(3):211–252, 2015.

[22] Mahmood Sharif, Sruti Bhagavatula, Lujo Bauer, and Michael K Reiter. Accessorize to a crime: Real and stealthy attacks on state-of-the-art face recognition. In *Proceedings of the 2016 ACM SIGSAC Conference on Computer and Communications Security*, pages 1528–1540, 2016.

[23] Christian Szegedy, Sergey Ioffe, Vincent Vanhoucke, and Alexander A Alemi. Inception-v4, Inception-ResNet and the impact of Residual Connections on learning. In *Proceedings of the Thirty-First AAAI Conference on Artificial Intelligence, AAAI*, 2017.

[24] Christian Szegedy, Vincent Vanhoucke, Sergey Ioffe, Jon Shlens, and Zbigniew Wojna. Rethinking the inception architecture for computer vision. In *IEEE Conference on Computer Vision and Pattern Recognition, CVPR*, pages 2818–2826, 2016.

[25] Christian Szegedy, Wojciech Zaremba, Ilya Sutskever, Joan Bruna, Dumitru Erhan, Ian Goodfellow, and Rob Fergus. Intriguing properties of neural networks. In *2nd International Conference on Learning Representations, ICLR*, 2014.

[26] Florian Tramèr, Alexey Kurakin, Nicolas Papernot, Ian Goodfellow, Dan Boneh, and Patrick McDaniel. Ensemble adversarial training: Attacks and defenses. In *6th International Conference on Learning Representations, ICLR*, 2018.

[27] Xiaosen Wang and Kun He. Enhancing the transferability of adversarial attacks through variance tuning. In *IEEE Conference on Computer Vision and Pattern Recognition, CVPR*, pages 1924–1933, 2021.

[28] Xiaosen Wang, Xuanran He, Jingdong Wang, and Kun He. Admix: Enhancing the transferability of adversarial attacks. In *Proceedings of the IEEE/CVF International Conference on Computer Vision, ICCV*, pages 16158–16167, 2021.

[29] Lei Wu, Zhanxing Zhu, Cheng Tai, et al. Understanding and enhancing the transferability of adversarial examples. *arXiv preprint arXiv:1802.09707*, 2018.

[30] Weibin Wu, Yuxin Su, Michael R. Lyu, and Irwin King. Improving the transferability of adversarial samples with adversarial transformations. In *IEEE Conference on Computer Vision and Pattern Recognition, CVPR*, pages 9024–9033, 2021.

[31] Cihang Xie, Jianyu Wang, Zhishuai Zhang, Zhou Ren, and Alan Yuille. Mitigating adversarial effects through randomization. In *6th International Conference on Learning Representations, ICLR*, 2018.

[32] Cihang Xie, Zhishuai Zhang, Yuyin Zhou, Song Bai, Jianyu Wang, Zhou Ren, and Alan L Yuille. Improving transferability of adversarial examples with input diversity. In *IEEE Conference on Computer Vision and Pattern Recognition, CVPR*, pages 2730–2739, 2019.

[33] Kaidi Xu, Gaoyuan Zhang, Sijia Liu, Quanfu Fan, Mengshu Sun, Hongge Chen, Pin-Yu Chen, Yanzhi Wang, and Xue Lin. Adversarial t-shirt! evading person detectors in a physical world. In *16th European Conference on Computer Vision, ECCV*, pages 665–681, 2020.

[34] Weilin Xu, David Evans, and Yanjun Qi. Feature squeezing: Detecting adversarial examples in deep neural networks. In *25th Annual Network and Distributed System Security Symposium, NDSS*, 2018.

[35] Zheng Yuan, Jie Zhang, Yunpei Jia, Chuanqi Tan, Tao Xue, and Shiguang Shan. Meta gradient adversarial attack. In *Proceedings of the IEEE/CVF International Conference on Computer Vision, ICCV*, pages 7748–7757, 2021.